Advanced Materials Research *Online: 2013-11-15*
ISSN: 1662-8985, Vol. 842, pp 564-568
doi:10.4028/www.scientific.net/AMR.842.564

Kinematics of a New 14 DOF Humanoid Biped Robot

Lumin Chen [a], Fan Wang [b]

College of Electromechanical Science and Engineering, Zhengzhou University of Light Industry, Zhengzhou, Henan, 450002, China

[a]luminchen@126.com, [b]wangfanzls@126.com

Keywords: Humanoid biped robot, 14 Degree-of-Freedom, Kinematic.

Abstract. This paper proposes a novel architecture for a biped robot with six DOFs per leg and an active toe DOF (Degrees of Freedom). The arrangement of three successive DOFs paralleled to each other makes its inverse kinematics simple and decoupled by omitting one DOF which is unnecessary when walking. And this work presents close equations for the forward and inverse kinematics. The results can be used in the kinematic control study of the robot.

Introduction

Research in the field of humanoid robotics has evolved greatly in the last few years. Although the efforts have mainly focused on achieving human gait, this feature has not been successful accomplished with a limited number of DOF.

Generally speaking, hip joint has three DOFs, including the pitch DOF, the yaw DOF and the roll DOF, in which the pitch DOF is needful when the robot taking a step forward; the yaw DOF is necessary when the center of gravity is shifting; and when the robot making a turn the roll DOF is useful. And the knee joint has a pitch DOF, which could adjust the height of the swing leg and make it possible to up and down the steps. Therefore, the difference of arrangement of the DOFs is that the number of DOF in ankle and toe joint, that is to say, whether there is a roll DOF in ankle joint and whether there is a toe joint or not. The following is several cases.

The first is robots with 6 DOFs per leg, such as HRP-3[1], KHR-3[2], and Johnnie [3], they have in common is the ankle joint has two DOFs: the pitch DOF and the yaw DOF. And the second is robots with legs of 6 DOFs + 1 DOF in the toe, for instance, H7 [4], and Lola [5], and they both have 2 DOFs in ankle joint and 1 DOF in toe joint. In addition, there are robots with 7-DOF legs without toe as WABIAN-2[6], and its ankle joint has 3DOFs. What's more, a more sophisticated robot has 8 DOFs with toe named HYDROÏD [7] has been designed, although conducive to make the walk more anthropomorphic, this structure is heavy and complex very much.

Different from the examples cited above, this paper suggests a new architecture for a biped robot with seven DOF per leg, as follows: 3 DOFs for the hip, 1 DOF for the knee, 2 DOFs for the ankle, and 1 DOF for the toe as shown in Fig. 1. Firstly, although there are only 2 DOFs in the ankle joint and the swerve is relied on the roll DOF of hip joint, this design reduce the complexity, and be beneficial to the organization arrangement of ankle joint, thus reduce the volume and quality of the lower limb robot, and it still can achieve the basic motion gait. Secondly the toe joint can make the lower limb robot achieve an approximate human gait motion and walk in a more natural manner.

The paper is organized as follows. In Section 2, the specific aspects of this humanoid biped robot are briefly presented. The forward kinematics for the proposed humanoid robot is obtained in Section 3. This is followed by Section 4, which focuses on the analytical solution of the inverse kinematic of the leg in the non-redundant case. Finally, Section 5 presents some important conclusions and suggestions for future research on this new architecture for a humanoid biped robot.

Mechanical design of the biped robot

This biped robot has three special aspects, as shown in Fig.1. First, one DOF that imitates the toe joint is added. Compared with conventional humanoid robots that are equipped with flat feet, the addition of an active toe joint to the kinematic model of each leg allows a robot not only to achieve an approximate human gait motion, but also to walk in a more natural manner.

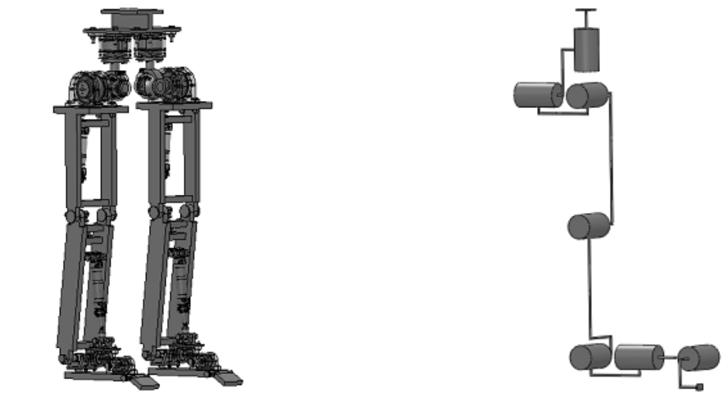

a. Mechanical design b. Arrangement of the DOFs

Fig. 1 Humanoid biped robot

Second, the design of its hip joint is different from those of other humanoid robots. Considering the fact that the rotation in the sagittal plane is the largest and heaviest of the three hip DOFs, this joint therefore is placed the last of the three so the other two DOFs do not carry the weight of it to improve the robot dexterity.

Third, the three DOFs with an axis perpendicular to the sagittal plane (q_3 for the hip, q_4 for the knee and q_5 for the ankle) are successive and parallel to each other. This complies with the Pieper's rule [8], therefore the closed-form solution can be got, and the calculation is more convenient and simple.

Forward Kinematics

In robotics literature, forward kinematics is commonly known as the task in which the position and orientation of the end effector is to be determined by giving the configurations for the active joints of the robot.

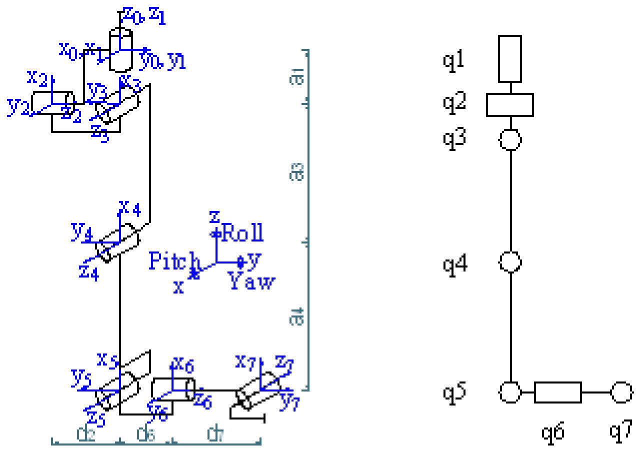

Fig. 2 Kinematic description of the robot leg

Table 1 Right leg DH parameter

DH parameter	Joint						
	1	2	3	4	5	6	7
θ_i	θ_1	θ_2	θ_3	θ_4	θ_5	θ_6	θ_7
α_i	0	-90°	-90°	0	0	90°	90°
a_i	0	$-a_1$	0	$-a_3$	$-a_4$	0	0
d_i	0	d_2	d_2	0	0	d_6	d_7

The local frames (X_i, Y_i, Z_i) are assigned to each joint according to the Denavit-Hartenberg (DH) convention. Since the general kinematic structures of the left leg of a humanoid robot are identical to those of the right leg, the paper assigns the same coordinate frames for the left and right limbs for convenience of analysis. Fig. 2 shows the designated local coordinate frames for the right leg, which consider the base frame (X_0, Y_0, Z_0) the same as the frame (X_1, Y_1, Z_1). And table 1 shows the DH parameters.

The position and orientation of the end-effector of a limb can be obtained by multiplying the link transformation matrices together, namely

$$ {}^{0}_{7}T = \prod_{i=1}^{7} {}^{i-1}_{i}T = {}^{0}_{1}T \cdot {}^{1}_{2}T \cdot {}^{2}_{3}T \cdot {}^{3}_{4}T \cdot {}^{4}_{5}T \cdot {}^{5}_{6}T \cdot {}^{6}_{7}T = \begin{bmatrix} n & o & a & p \\ 0 & 0 & 0 & 1 \end{bmatrix}. \quad (1)$$

Where ${}^{i-1}{}_{i}T$ is a general link transformation matrix relating the *i-th* coordinate frame to the *(i-1)th* coordinate frame, *n, o, a* represents the orientation vector, and *p* describes the position vector of the foot. According to the DH coordinate system, the homogeneous transformation of the link gives

$$ {}^{i-1}_{i}T = \begin{bmatrix} c\theta_i & -s\theta_i \cdot c\alpha_i & s\theta_i \cdot s\alpha_i & a_i \cdot c\theta_i \\ s\theta_i & c\theta_i \cdot c\alpha_i & -c\theta_i \cdot s\alpha_i & a_i \cdot s\theta_i \\ 0 & s\alpha_i & c\alpha_i & d_i \\ 0 & 0 & 0 & 1 \end{bmatrix}. \quad (2)$$

Where, $s\theta_i = \sin\theta_i$, $c\theta_i = \cos\theta_i$, $s\alpha_i = \sin\alpha_i$, $c\alpha_i = \cos\alpha_i$ .Furthermore, by using Eq. (1) and (2), the toe position vector results in

$$p_x = c_1 s_2 \left(d_7 s_{345} + d_6 s_{345} - a_4 c_{34} - a_3 c_3\right) - s_1 \left(d_7 c_{345} + d_6 c_{345} + a_4 s_{34} + a_3 s_3\right). \quad (3)$$

Where, $s_{ijk} = \sin(\theta_i + \theta_j + \theta_k)$, $c_{ijk} = \cos(\theta_i + \theta_j + \theta_k)$.

$$p_y = s_1 s_2 \left(d_7 s_{345} + d_6 s_{345} - a_4 c_{34} - a_3 c_3\right) + c_1 \left(d_7 c_{345} + d_6 c_{345} + a_4 s_{34} + a_3 s_3\right). \quad (4)$$

$$p_z = c_2 \left(d_7 s_{345} + d_6 s_{345} - a_4 c_{34} - a_3 c_3\right) - a_1. \quad (5)$$

Once the forward kinematics is obtained, the next section presents the solution to the inverse kinematic for the legs.

Inverse Kinematics

This section is concerned with finding the solution to the inverse kinematic problem, which consists of determining the joint variables in terms of the end effector position and orientation. There are two cases of the inverse kinematic: the first is when the leg lifted, the toe joint q7 which is not available can be omitted (see Figs. 3 and 5); the second is when the foot falling to the ground, q1can be omitted (see Figs. 4 and 6). Thus, the inverse kinematic problem related to the redundant will solved by using the two non-redundant models.

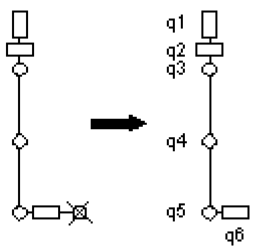

Fig. 3 Kinematic chain 1 (omitting q_7)

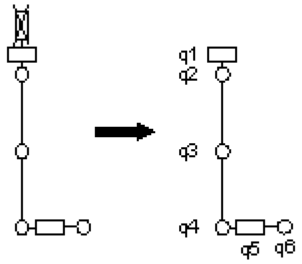

Fig. 4 Kinematic chain 2 (omitting q_1)

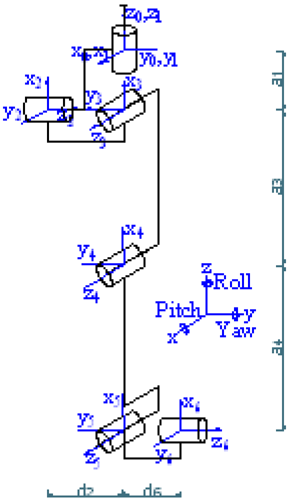

Fig. 5 Kinematic chain 1

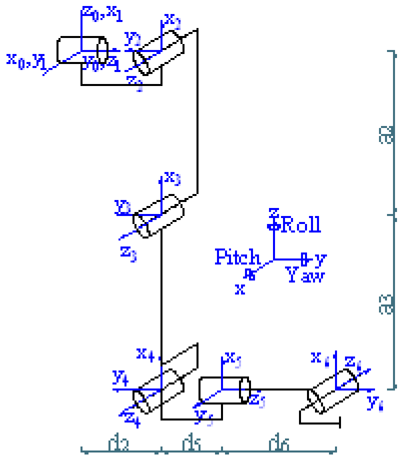

Fig. 6 Kinematic chain 2

4.1 Kinematic chain 1 (omitting q_7). Forward kinematics calculation of kinematic chain 1 (see Figs. 3, 5) can refer to the whole leg's forward kinematics calculation in section 3, rewrite Eq.1 into Eq.6 firstly

$$ {}^{0}_{6}T = \begin{bmatrix} n & o & a & p \\ 0 & 0 & 0 & 1 \end{bmatrix} = {}^{0}_{1}T \cdot {}^{1}_{2}T \cdot {}^{2}_{3}T \cdot {}^{3}_{4}T \cdot {}^{4}_{5}T \cdot {}^{5}_{6}T \,. \tag{6} $$

In Eq. 6, each element of the left matrix is known, although the six matrix of right which relies on the joint variables $\theta_{1,\cdots,}\theta_6$ is unknown. To get the unknown joint variable, using the unknown inverse transformation pre-multiply by the matrix equation in successive, this is convenient for separating a joint variable. In this way, the joint variables $\theta_{1,\cdots,}\theta_6$ can be determined as follows,

$$ \theta_1 = \mathrm{Atan2}\left(\frac{a_x}{a_z} - \frac{p_x}{p_z + a_1}, -\frac{a_y}{a_z} + \frac{p_y}{p_z + a_1}\right). \tag{7} $$

$$ \theta_2 = \mathrm{Atan2}\left(c_1 p_x + s_1 p_y, p_z + a_1\right). \tag{8} $$

$$ \theta_3 = \mathrm{Atan2}(w, \pm\sqrt{p^2 + q^2 - w^2}) - \mathrm{Atan2}(p, q)\,. \tag{9} $$

Where $p = (c_1 s_2 p_x + s_1 s_2 p_y + c_2 p_z + c_2 a_1) - d_6 (c_1 s_2 a_x + s_1 s_2 a_y + c_2 a_z)$,

$q = (s_1 p_x - c_1 p_y) - d_6 (s_1 a_x - c_1 a_y)$, $w = (a_4^2 - a_3^2 - p^2 - q^2)/(2a_3)$.

$$ \theta_4 = \arccos[(p^2 + q^2 - a_4^2 - a_3^2)/(2a_3 a_4)]. \tag{10} $$

$$ \theta_5 = \mathrm{Atan2}\begin{pmatrix} (c_1 s_2 c_{34} + s_1 s_{34}) a_x + (s_1 s_2 c_{34} - c_1 s_{34}) a_y + c_2 c_{34} a_z, \\ (c_1 s_2 s_{34} - s_1 c_{34}) a_x + (s_1 s_2 s_{34} + c_1 c_{34}) a_y + c_2 s_{34} a_z \end{pmatrix}. \tag{11} $$

$$ \theta_6 = \mathrm{Atan2}\begin{pmatrix} c_1 c_2 n_x + s_1 c_2 n_y - s_2 n_z, \\ (c_1 s_2 c_{345} + s_1 s_{345}) n_x + (s_1 s_2 c_{345} - c_1 s_{345}) n_y + c_2 c_{345} n_z \end{pmatrix}. \tag{12} $$

At this point, the inverse kinematics calculation of kinematic chain 1 is finished.

4.2 Kinematic chain 2 (omitting q_1). The inverse kinematics calculation of kinematic chain 2 (see Figs. 4 and 6) is the same as kinematic chain 1, and the joint variables $\theta_{1,\cdots,}\theta_6$ can be got as follows,

$$ \theta_1 = \mathrm{Atan2}(p_x, p_z)\,. \tag{13} $$

$$ \theta_3 = \arccos[(u^2 + v^2 - a_3^2 - a_2^2)/(2a_2 a_3)]. \tag{14} $$

Where $u = s_1p_x + c_1p_z - d_6s_{234} - d_5s_{234}$, $v = p_y - d_6c_{234} - d_5c_{234} - d_2$.

$$\theta_{234} = \text{Atan2}[-a_y, s_1a_x + c_1a_z]. \tag{15}$$

$$\theta_2 = \text{Atan2}(u, \pm\sqrt{(a_3c_3 + a_2)^2 + a_3^2s_3^2 - u^2}) + \text{Atan2}(a_3c_3 + a_2, a_3s_3). \tag{16}$$

$$\theta_4 = \theta_{234} - \theta_3 - \theta_2. \tag{17}$$

$$\theta_5 = \text{Atan2}(s_1c_{234}a_x - s_{234}a_y + c_1c_{234}a_z, -c_1a_x + s_1a_z). \tag{18}$$

$$\theta_6 = \text{Atan2}\begin{pmatrix} s_1s_{234}n_x + c_{234}n_y + c_1s_{234}n_z, \\ (s_1c_{234}c_5 + c_1s_5)n_x - s_{234}c_5n_y + (c_1c_{234}c_5 - s_1s_5)n_z \end{pmatrix}. \tag{19}$$

At this point, the inverse kinematics calculation of kinematic chain 2 is finished.

Conclusions and outlook

This paper presented a new architecture for a biped robot with six DOFs per leg and an additional DOF that imitates the toe joint, in which there are three successive DOFs paralleled to each other. First, the work presented the forward kinematic using the DH convention. Secondly, the inverse kinematics was approached by omitting one DOF in two cases.

Further work after this paper will focus on the workspace analysis, in order to determine the real motion range of this lower limb robot. Followed by is the dynamics simulated analysis by ADAMS, and the simulation results provide the basis for optimization structure and parameters of robot and the trajectory planning and control.

References

[1] K. Kaneko, K. Harada, F. Kanehiro, G. Miyamori, K. Akachi, Humanoid robot hrp-3, Proc. IEEE/RSJ International Conference on Intelligent Robots and System, 2008, pp: 2471-2478.

[2] I. -W. Park, J. -Y. Kim, J. Lee, J. -H. Oh, Mechanical design of the humanoid robot platform, hubo, Advanced Robotics 21 (2007) 1305-1322.

[3] K. Loffler, M. Gienger, F. Pfeiffer, Sensors and control concept of walking “johnnie”, International Journal of Robotics Research 22 (2003) 229-239.

[4] K. Nishiwaki, J. Kuffner, S. Kagami, M. Inaba, H. Inoue, The experimental humanoid robot h7: a research platform for autonomous behavior, Philosophical Transactions of the Royal Society A: Mathematical, Physical and Engineering Sciences 365 (2007) 79-107.

[5] T. Buschmann, S. Lohmeier, H. Ulbrich, Humanoid robot lola: Design and walking control, Journal of Physiology, Paris 103 (3-5) (2009).

[6] Y. Ogure, H. Aikawa, K. Shimomura, A. Morishima, H.ok Lim, A. Takanishi, Development of a new humanoid robot wabian-a, Proc. IEEE International Conference on Robotics and Automation, 2006, pp: 76-81.

[7] S. Bertrand, O. Bruneau, F. B. Ouezdou, S. Alfayad. Closed-form solutions of inverse kinematic models for the control of a biped robot with 8 active degrees of freedom per leg. Mechanism and Machine Theory 49 (2012) 117–140.

[8] Pieper D L .The kinematics of manipulators under computer control. [D] Stanford: Stanford University, 1968.